

High-Sensitivity Stable-Isotope Probing by a Quantitative Terminal Restriction Fragment Length Polymorphism Protocol

Peter Andeer,^a Stuart E. Strand,^a and David A. Stahl^{a,b}

Department of Civil and Environmental Engineering, University of Washington, Seattle, Washington, USA,^a and Department of Microbiology, University of Washington, Seattle, Washington, USA^b

Stable-isotope probing (SIP) has proved a valuable cultivation-independent tool for linking specific microbial populations to selected functions in various natural and engineered systems. However, application of SIP to microbial populations with relatively minor buoyant density increases, such as populations that utilize compounds as a nitrogen source, results in reduced resolution of labeled populations. We therefore developed a tandem quantitative PCR (qPCR)–TRFLP (terminal restriction fragment length polymorphism) protocol that improves resolution of detection by quantifying specific taxonomic groups in gradient fractions. This method combines well-controlled amplification with TRFLP analysis to quantify relative taxon abundance in amplicon pools of FAM-labeled PCR products, using the intercalating dye EvaGreen to monitor amplification. Method accuracy was evaluated using mixtures of cloned 16S rRNA genes, DNA extracted from low- and high-G+C bacterial isolates (*Escherichia coli*, *Rhodococcus*, *Variovorax*, and *Microbacterium*), and DNA from soil microcosms amended with known amounts of genomic DNA from bacterial isolates. Improved resolution of minor shifts in buoyant density relative to TRFLP analysis alone was confirmed using well-controlled SIP analyses.

Since its introduction, stable-isotope probing (SIP) has served as a valuable technique for linking microbial function to community structure by identifying populations that metabolize selected substrates (7, 18, 22, 31). In SIP, the system of interest is first challenged with a substrate labeled with a stable isotope, usually a heavier isotope of carbon (¹³C) or nitrogen (¹⁵N). Then, DNA or RNA from organisms that have incorporated the isotope are separated from unlabeled nucleic acid by cesium chloride (CsCl) or cesium trifluoroacetate (CsTFA) density gradient centrifugation (23, 27), respectively. Populations that have incorporated label are identified by comparative analysis of gradient fractions containing heavy and light DNA, generally by selective amplification and sequencing of specific genes (32), fingerprinting techniques such as terminal restriction fragment length polymorphism (TRFLP) analysis (7, 22, 36) and denaturing gradient gel electrophoresis (DGGE) (15, 23, 33), or metagenomic analysis (18, 26, 37).

The most statistically robust conclusions are derived from simple presence-or-absence analysis, for example, as determined by using diagnostic TRFLP fragments (10). However, presence-absence assessment is dependent upon complete separation of heavy and light DNA. For this reason, with some notable exceptions (6, 7, 36, 41), most analyses have focused on substrates labeled with ¹³C, offering better resolution of labeled and unlabeled nucleic acids than can be achieved with the smaller increases in buoyant density (BD) from ¹⁵N incorporation (1, 11). In particular, small changes in density with ¹⁵N incorporation may not be sufficient to differentiate labeled DNA from unlabeled DNA of high G+C content (1, 6, 8, 11). Although analysis can be improved by using AT-selective intercalating dyes which exaggerate G+C bias (6, 7, 19), because the distribution of nucleic acids is Gaussian (28), nucleic acids derived from an abundant population are often distributed throughout a gradient. Thus, TRFLP analysis alone may not be sufficient for accurate determination of peak position within a gradient or for comparisons of gradients containing variable amounts of DNA.

To address this limitation, we developed a general protocol for

accurate determination of peak position by combining a fluorophore-labeled primer with an intercalating dye to quantify individual TRFLP restriction fragments (RFs) in individual fractions of the gradient. The intercalating dye is used for real-time monitoring of amplification so reactions can be terminated before amplification efficiency is compromised by reaction component limitations (40). The fluorophore label is subsequently employed to quantify individual RFs. Importantly, the method is not constrained by the requirement for an additional internal hybridization site, as required for the TaqMan protocol (43), providing greater flexibility in the design of primers used to assess sequence diversity.

MATERIALS AND METHODS

Figure 1 presents an overview of the developed tandem qPCR–TRFLP protocol for SIP analysis. The experiments conducted to validate the protocol are described below.

Construction of 16S rRNA gene standards. DNA standards for TRFLP analysis with minimal sequence variation near the qPCR priming sites were constructed for the initial experiments. Bacterial primers 27F and 1492R were used to amplify near-complete 16S rRNA gene sequences from *Flavobacterium* sp., *Acidovorax* sp., *Arthrobacter* sp., and *Microbacterium* sp. chromosomal DNA (21) and ligated into the Invitrogen pCR4 vector (Life Technologies; Carlsbad, CA). Plasmids containing the cloned fragments were extracted using the Qiagen plasmid miniprep kits (Qiagen, Valencia, CA) following the manufacturer's instructions, quantified by triplicate *A*₂₆₀ measurements using a NanoDrop ND-1000 spectrophotometer (ThermoFisher Scientific; Wilmington, DE), and stored as 25-ng

Received 24 June 2011 Accepted 14 October 2011

Published ahead of print 28 October 2011

Address correspondence to Stuart E. Strand, sstrand@u.washington.edu.

Supplemental material for this article may be found at <http://aem.asm.org/>.

Copyright © 2012, American Society for Microbiology. All Rights Reserved.

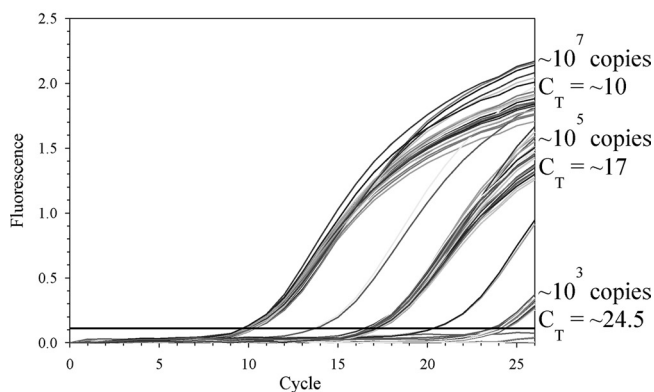
doi:10.1128/AEM.05973-11

Tandem qPCR-TRFLP analysis of CsCl gradients

Step 1. DNA extraction, SIP separation, fractionation and purification



Step 2. Fractions amplified, quantified with SsoFast EvaGreen Supermix using a fluorescently-labeled 16S primer set: [FAM]-27F, 338R.



qPCR reactions terminated in exponential phase (e.g., the samples ca. 10^3 copies in the inserted image) to minimize # of cycles and associated bias



Step 3. qPCR product purified, digested (MspI and MnlI), and separated on an ABI 3730 DNA Analyzer



Step 4. Individual RF abundance calculated from qPCR of total 16S rRNA gene copy numbers.

$$\text{RF copy number} = \text{total copy numbers} * \text{RF fraction}$$



Step 5. Copy numbers of each RF plotted against buoyant density for each gradient.

¹⁵N-SIP profiles are compared to unlabeled controls to identify assimilating populations.

FIG 1 Tandem qPCR-TRFLP analysis of CsCl gradients. The flow diagram shows the steps used to assign quantities for individual RFs (steps 2 to 4) and how these calculations are used in SIP analysis.

μl^{-1} stock solutions. Mixes of 16S rRNA gene clones from the four species were prepared at various gene copy ratios (from equimolar to 10:1:1:1; see Table S1 in the supplemental material).

Preparation of pure culture genomic DNA. The influence of sequence variation on amplification efficiency was examined using DNA extracted from pure cultures of both high- and low-G+C organisms. *E. coli* K-12 MG1655, *Rhodococcus rhodochrous* 11Y, *Microbacterium* sp.

MA1, and *Variovorax* sp. were grown on the previously described (3) minimal medium used for enrichment of 1,3,5-trinitro-1,3,5-triazine (RDX)-degrading organisms with either RDX, 99% [^{15}N]RDX (Defense Research and Development Canada, Valcartier, QC, Canada), ammonium nitrate, or 98% [^{15}N]ammonium [^{15}N]nitrate (Sigma-Aldrich; St. Louis, MO) supplied as a nitrogen source. Genomic DNA mixtures were prepared from pure cultures as described previously, with the exception that sucrose was not used in the lysis solution (3). DNA for the SIP experiment was prepared using the soil extraction protocol described below, excluding aluminum sulfate incubation.

Soil microcosms. Soil microcosms were established to provide a diverse, undefined source of DNA for the mock SIP experiment and method development. Soil slurries containing 13% (wt/vol) soil were incubated for 3.5 days with an enrichment medium for RDX degraders (3). RDX degradation was monitored using the previously described high-pressure liquid chromatography method (3).

DNA extraction from soil microcosms. DNA was extracted from soil slurries using a modification of a previously published protocol by incorporating a preincubation step with aluminum sulfate to remove humic acids (13). Approximately 300 mg of soil was loaded into a lysing matrix E tube (MP Biomedicals; Solon, OH) with 130 μl of 100 mM AlSO_4 solution (pH 3), 200 μl of 100 mM sodium phosphate buffer (pH 6.6), 60 μl of 1 M NaOH (to pH \sim 9.0), 560 μl of extraction buffer (55 mM NaPO_4 , 225 mM Tris, 100 mM NaCl [pH \sim 8.5]), and 160 μl of 20% sodium dodecyl sulfate (SDS) solution. The samples were disrupted in a FastPrep 1200 bead beater (MP Biomedicals) for 30 s at a machine setting of 4.0 and centrifuged for 10 min at $16,000 \times g$, and the supernatant was transferred to a clean microcentrifuge tube on ice. Concentrated HCl (2 μl) was then added to the soil pellet, and extraction was repeated using a 200 mM AlSO_4 solution and volumes of all reagents that were 50% of those used in the initial extraction. After centrifugation, the supernatants were combined, incubated on ice or at -20°C for 20 min, and centrifuged for 10 min at $20,000 \times g$ at 4°C to remove excess SDS. A 0.2 volume of 5 M NaClO_4 (pH 9) was added to the combined supernatants, and the mixture was incubated for 10 min at 55°C . Following two extractions with cold CIA (chloroform-isoamyl alcohol, 24:1), nucleic acids were recovered by the addition of 1 volume isopropanol and washed using standard protocols (35).

Isopycnic centrifugation and gradient fractionation. DNA (\sim 4.9 μg) recovered from a soil microcosm using the described protocol was added to a mixture of unlabeled or ^{15}N -labeled genomic DNA (\sim 620 to 670 ng) from *E. coli* K-12 MG1655, *Rhodococcus rhodochrous* 11Y, and *Microbacterium* sp. MA1. The combined DNA was then added to a TE/CsCl solution (10 mM Tris, 10 mM EDTA [pH 8.0], CsCl to a BD [buoyant density] of 1.71 g ml^{-1}) with a volume of 4.8 ml in OptiSeal polyallomer tubes (Beckman Coulter, Brea, CA) and a final BD of \sim 1.67 g ml^{-1} based on density measurements. Gradients were established in a TLA110 rotor run for 96 h at 55,000 rpm in an OptimaMax ultracentrifuge (Beckman Coulter) (6). Gradients were then displaced with light mineral oil pumped into the top of the tube, collecting 90 to 105 μl fractions dropwise from a point near the bottom of the tube. The BD of each fraction was determined using a modified AR200 digital refractometer (Reichert, Ithaca, NY) as described by Buckley et al. (6). To account for possible measurement error, fraction number was plotted against buoyant density and fitted with a linear curve for analysis. Fractions were combined, concentrated, and dialyzed against DNA suspension buffer (10 mM Tris, 0.1 mM EDTA [pH 8.0]) using 30-kDa Microcon membrane spin filters (Millipore, Billerica, MA) centrifuged at $6,000 \times g$. Eluates were all adjusted to 60 μl by addition of the same buffer.

Quantitative PCR. Amplification products for TRFLP analyses were produced and quantified using the following protocol. qPCR (20 μl) consisted of 10 μl of SsoFast EvaGreen supermix (Bio-Rad, Hercules, CA), 6.4 μl of PCR certified water (Teknova, Hollister, CA), 8 pmol each of the 6'-carboxyfluorescein (6'-FAM)-labeled primer 27F (Eurofins MWG Operon; Huntsville, AL) and unmodified primer 338R (2), and 2 μl of

TABLE 1 Effect of fluorescein labeled primer 6'-FAM-27F on qPCR standard curve values^a

Primer	Threshold ^b	Slope ^c	Intercept ^c	R ^{2c}	Copy no. for MA1		Coefficient of variation (%)
					Avg	SD	
27F	0.016	-3.51	34.0	1.00	6.48E + 04	8.19E + 03	12.64
6'-FAM-27F	0.154	-3.57	37.4	1.00	5.50E + 04	7.42E + 03	13.51

^a Data were generated from *E. coli* and copy number calculations for *Microbacterium* sp. MA1 using either 27F or 6'-FAM-27F with 338R. *E. coli* genomic DNA was diluted from 10⁷ to 10³ copies of the 16S rRNA gene per μ l, and MA1 copy number statistics were generated using threefold dilutions of the DNA within the standard curve's range. Amplifications were performed in duplicate under the same cycling conditions.

^b Threshold value used for C_T calculation in respective quantifications.

^c Standard curve [log(gene copy no.) versus C_T].

template DNA or water. PCR and amplification monitoring was run in duplicate for each dilution using an MJ-Research PTC-200 gradient thermocycler with a Chromo 4 real-time PCR detector with Opticon Monitor 3.1 software (Bio-Rad). Initial denaturation was performed at 98°C for 2 min, and each cycle was 98°C for 8 s, 58°C for 12 s, and 72°C for 15 s, with a 5-min final extension step added after cycling was finished. A dilution series from 250 pg μ l⁻¹ to 2.5 fg μ l⁻¹ of *Flavobacterium* sp. 16S rRNA gene clones (4.3 × 10⁷ to 4.3 × 10² copies μ l⁻¹) was used to generate a standard curve for quantification of 16S rRNA gene clones. For genomic DNA and spiked soil samples, *E. coli* K-12 MG1655 from 25 ng μ l⁻¹ to 250 fg μ l⁻¹ (3.44 × 10⁷ to 3.44 × 10² copies μ l⁻¹) was used for standard curve generation to avoid the overestimation of the copy numbers that can occur when plasmids are used for standards (17). To estimate 16S rRNA gene quantities in DNA extracted from pure cultures and soils, qPCR was performed on serial dilutions of the genomic DNA in multiple qPCRs.

Purified density gradient fractions were purified as described above, and an initial amplification was performed to estimate concentration in each fraction. Fractions were then amplified in batches based on threshold cycle (C_T) (each sample in duplicate or triplicate) values so that amplification could be terminated in exponential phase. The Opticon software was used for analysis with subtraction of global minimum baselines and without curve smoothing. Threshold fluorescence levels were set to the lowest levels that minimize error in standard curves, typically at values between 0.1 and 0.15. Slopes and R² values of semilog regression curves of the standards were routinely -3.3 ± 0.3 and >0.99, respectively.

TRFLP sample preparation and processing. qPCR products were purified using a PSIClone HTS PCR 96 purification kit (Princeton Separations, Freehold, NJ) following the manufacturer's instructions. DNA was digested with 0.5 μ l each of FastDigest MnlI and MspI enzymes (Fermentas; Glen Burnie, MD) for 1 h, followed by a second addition of enzyme and incubation from 2 h to overnight. Digests were purified by addition of phenol chloroform followed by centrifugation, and 20 μ l of supernatant was applied to Centrisep 96 plates (Princeton Separations). Aliquots (4 μ l) of properly diluted reaction mixtures were mixed with 12.5 μ l of HiDi formamide and 0.2 μ l of ROX-labeled custom Mapmarker (30, 50, 100, 150, 200, 250, 300, 400, 500, 510, and 550 bp; Bioventures, Murfreesboro, TN). Samples were processed on an Applied Biosystems 3730 DNA analyzer (Life Technologies).

Data analysis. Analysis of TRFLP profiles was performed using DAX data acquisition and analysis software, v7.0 (Van Mierlo Software Consultancy, Eindhoven, The Netherlands). Peaks were binned manually, and quantification of peaks was performed based on both relative area and relative height of the peaks when normalized to total profile area or total profile height, respectively.

DNA sequencing. 16S rRNA gene sequences originating from this work were amplified using the bacterial primers 27F and 1492R (21), ligated into the pCR4 vector (Invitrogen), and transformed using a TOPO-TA cloning kit (Invitrogen), and recombinant colonies were submitted directly to High-Throughput Sequencing Solutions (www.htseq.org). The GenBank accession numbers for the partial 16S rRNA gene sequences of *E. coli* K-12 MG1655 (5), *R. rhodochrous* 11Y (38) and *Microbacterium* sp. MA1 (3) are NC_000913, AF439261, and FJ357539, respectively.

Nucleotide sequence accession numbers. The accession numbers for the partial 16S rRNA sequence clones used in the plasmid tests are JN983794, JN983795, JN983796, and JN983797. The accession number for the *Variovorax* 16S rRNA sequence used in the tests with genomic DNA is JN983798.

RESULTS

Because a linear relationship between fluorescence intensity and target sequence abundance could be achieved by early termination of the amplification reaction (Fig. 1), the relative copy number of each RF corresponds to the relative fluorescence intensity. Several initial tests were performed to validate this equivalency. The effects of replacing a typical primer in the qPCR with a fluorescein-labeled primer (Fig. 1, step 2) were first analyzed. Then, a series of experiments were conducted to develop and evaluate the method of calculating the copy numbers associated with individual RF values (Fig. 1, step 4). Finally, a mock SIP experiment was conducted to demonstrate the improvement in resolution of density-shifted populations obtained with this method versus a TRFLP analysis alone.

The influence of the fluorescein-labeled primer on qPCR quantification was investigated by comparing standard curves developed for DNA from *E. coli* (3.44 × 10⁷ to 3.44 × 10³ 16S rRNA gene copies μ l⁻¹) and *Microbacterium* sp. MA1 (170 pg ml⁻¹, 17 pg ml⁻¹, and 1.7 pg ml⁻¹). Following amplification with either 27F or 6'-FAM-27F paired with 338R, the threshold was set empirically to maximize R² for the standard curve, subtracting the global minimum baseline. Table 1 shows a comparison of the standard curves [log(gene copy number) versus C_T] parameters, as well as the average calculated copy numbers, for the MA1 DNA. The major difference between the two data sets is the increased threshold used to calculate C_T values (0.154 versus 0.016) for the FAM-labeled primer amplification due to the FAM background fluorescence. Nonetheless, the parameters and calculations generated at the respective threshold values with the fluorescent primer were very close to those obtained with the unlabeled primer.

The effects of DNA concentration and amplification cycles on RF quantification were initially examined using mixtures of plasmids and mixtures of pure culture DNA. Two RF quantification methods were evaluated: relative peak areas and relative peak heights. The accuracy of the various qPCR conditions and RF quantification methods were compared through linear regressions of the quantities added versus the quantities detected.

The four plasmids, or 16S rRNA gene standards, consisted of the pCR4 vector containing either a *Flavobacterium* sp., *Arthrobacter* sp., *Microbacterium* sp., or *Acidovorax* sp. 16S rRNA gene sequence, having RFs of 44, 150, 156, and 280 bp, respectively. Ten mixtures of the reference plasmids were prepared in ratios ranging from 1:1:1:1 to 10:1:1:1 (see Table S1 in the supplemental mate-

TABLE 2 Consistency between predetermined compositions of DNA mixtures and qPCR-TRFLP quantification of the compositions under varied amplification^a

Template DNA	16S rRNA gene copy no. ^b	Avg C_T	No. of qPCR cycles	Linear regression values					
				Area ^c			Height ^d		
				Slope	Intercept	R^2	Slope	Intercept	R^2
Plasmid mixtures	10^6	13	16	1.03	-0.75	0.97	1.02	-0.56	0.99
	10^7	10	16	0.93	1.74	0.93	0.94	1.46	0.95
	10^3	24.5	26	0.81	4.8	0.84	0.84	4.12	0.89
	10^5	17	26	0.80	4.97	0.90	0.80	5.04	0.97
	10^7	10	26	0.65	8.86	0.84	0.71	7.39	0.93
Genomic DNA mixtures	10^6	13	19	0.92	2.02	0.98	0.91	2.74	0.98
	10^5	16.5	19	1.00	-0.96	0.99	1.01	-0.30	0.99

^a Concentrations and cycle amplifications were varied from 10^3 to 10^7 gene copies/ μl and 16 to 26 cycles for gene standards and 10^5 to 10^6 gene copies/ μl and 19 cycles for genomic DNA respectively (see the supplemental material). The results of each of the four gene standards were plotted together at each condition (60 to 104 data points per plot). Similarly, the data points for each genomic DNA dilution (45 and 51) were plotted together.

^b Plasmid mixtures and genomic DNA mixtures were quantified with 16S rRNA gene standards and *E. coli* genomic DNA, respectively.

^c Linear regression values are the percentage added versus the TRFLP percentage, calculated as RF area divided by total chromatogram area. Intercept units are number of copies detected μl^{-1} , and slope units are number of copies detected per calculated copy.

^d Linear regression values are the percentage added versus the TRFLP percentage, calculated as RF height divided by total chromatogram height. Intercept units are number of copies detected μl^{-1} , and slope units are number of copies detected per calculated copy.

rial), diluted to concentrations between $250 \text{ pg } \mu\text{l}^{-1}$ and $25 \text{ fg } \mu\text{l}^{-1}$, and amplified using either 16 or 26 temperature cycles. Table 2 presents the linear regression values for the relative RF quantities of the plasmids. Linear regressions were performed on plasmid RF quantities combined based on DNA quantity and number of amplification cycles.

Although 16S rRNA gene ratios were generally comparable when either relative peak areas or relative peak heights were used, calculations based on RF peak heights provided greater precision and accuracy. The best quantification of the plasmid mixture RFs, i.e., slopes closest to 1.00 and intercepts closest to 0.00, was observed in the samples amplified with the fewest cycles and terminated in mid-exponential phase (3 cycles beyond its threshold cycle) (Table 2). The accuracy decreased slightly when the reaction was terminated in late exponential phase. Linear regression slopes, intercepts, and R^2 values were poorer at higher template concentrations (10^7 copies μl^{-1} versus 10^6 copies μl^{-1}) (Table 2) and when amplification was extended from 16 to 26 cycles. These findings illustrate the importance of terminating amplification in exponential phase for accurate quantification of RFs.

Table 2 also presents linear regression parameters derived from RF quantification of genomic DNA from the low-G+C *E. coli* and the high-G+C organisms, *Variovorax* sp. and *Rhodococcus rhodochrous* 11Y. Genomic DNA from these three isolates was amplified alone and in mixtures in which each species accounted for 10% to 80% of the 16S rRNA gene copy numbers (see Table S2 in the supplemental material). In the absence of corresponding genome sequences, the numbers of 16S rRNA gene copies per ng of DNA for *Variovorax* sp. (4.04×10^5 ; standard deviation [SD], 2.4×10^4) and *Rhodococcus rhodochrous* (2.75×10^5 ; SD, 2×10^4) were estimated using *E. coli* DNA as a qPCR standard. The 16S rRNA gene copy numbers of three *Rhodococcus* strains and six *Comamonadaceae* family members available in the Microbesonline.org database (12) ranged from 6.58×10^5 to 1.44×10^6 copies per ng DNA for *Rhodococcus* and 9.46×10^5 and 1.68×10^6 copies per ng for the *Comamonadaceae* (see Table S3 in the supplemental material). TRFLP profiles from all three species generated primary and secondary RF peaks that were verified *in silico* and summed for

abundance calculations. *E. coli* had primary and secondary peaks at 122 bp and 172 bp, *Variovorax* sp. at 231 bp and 273 bp, and *R. rhodochrous* at 158 bp and 168 bp, respectively. When amplification was terminated closer to the C_T values, better correlations were observed. Nonetheless, both dilutions correlated well, having R^2 values greater than 0.98 regardless of dilution or calculation metric, along with slopes above 0.9 and intercepts less than 3 detected copies μl^{-1} in all cases (Table 2).

Quantification using the qPCR-TRFLP method was then evaluated using a more complex template mixture. TRFLP profiles were generated using soil microcosm DNA amended with various amounts of DNA from pure cultures of *E. coli*, *Variovorax* sp., or *R. rhodochrous* 11Y (comprising 5% to 80% of total DNA) (see Table S4 in the supplemental material). Each amended sample was then analyzed at three dilutions ($25 \text{ ng } \mu\text{l}^{-1}$ to $25 \text{ fg } \mu\text{l}^{-1}$). As inferred from the slopes of the soil DNA and diluted genomic DNA, amplification efficiency was between 87% and 101% (ca. -3.3 to -3.7 copies detected per copy calculated).

Copy numbers of the 16S rRNA genes determined for the soil extract alone (5.08×10^5 copies ng^{-1} ; SD, 1.3×10^5) were used to calculate the number of copies of added DNA. Linear regressions of the calculated copy numbers versus the RF copy numbers all had slopes above 0.69 and in most cases R^2 values above 0.96 (see Table S5 in the supplemental material). Instances of lower correlation may be attributable to variation in amplification efficiency between the various populations due to differences in G+C content and sequence variability around priming sites (30). For example, quantification of *E. coli* DNA was better at 25 amplification cycles, whereas quantification of high-G+C bacteria was better at 32 amplification cycles (see Table S5). Additional analyses of these mixtures at different concentrations and amplification cycles were comparable (see Tables S4 and S5 and Fig. S1 in the supplemental material). TRFLP analysis of the soil DNA (data not shown) revealed small RFs corresponding to the genomic DNA RFs, accounting for the increase in intercept values from zero.

Finally, the optimized qPCR-TRFLP method was used to determine shifts in buoyant density (BD) of individual operational taxonomic units (OTUs), which are diagnostic of stable isotope

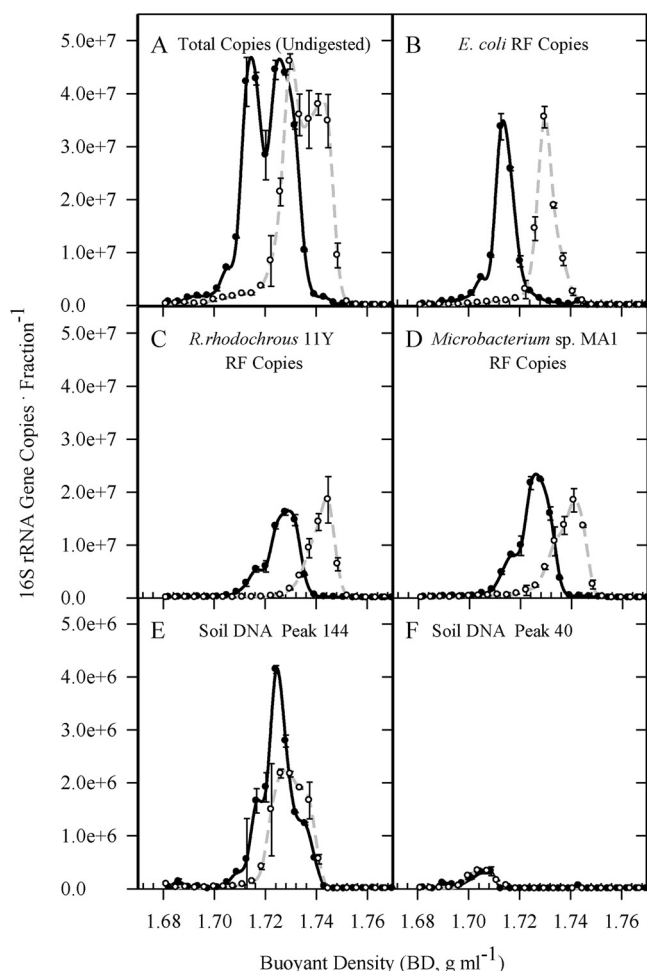


FIG 2 qPCR-TRFLP analysis of 16S rRNA genes in SIP fractions. (A) 16S rRNA gene copies (FAM-27F and 338R) per fraction of the CsCl gradients with soil DNA amended with unlabeled genomic DNA (solid line) and ^{15}N -genomic DNA (dashed line). (B to D) Profiles of unlabeled (solid line) and ^{15}N -labeled (dashed line) 16S rRNA gene fragment copies of *E. coli*, *R. rhodochrous* 11Y, and *Microbacterium* sp. MA1. (E and F) 16S rRNA gene copy profiles of two RF fragments from the unlabeled soil DNA in the two gradients. The data in panels B to F were generated from TRFLP analysis of digested (MnII and MspI) qPCR products (A); RF copies per fraction were calculated from relative peak heights multiplied by full copy number. Error bars are standard deviations for duplicate qPCR (A) and calculated RF quantities (B to F).

assimilation. DNA isolated from a soil microcosm was combined with a known mixture of ^{15}N -labeled genomic DNA from *Microbacterium* sp. MA1, *Rhodococcus rhodochrous* 11Y (high G+C), and *E. coli* (low G+C). A reference gradient contained the soil DNA and unlabeled genomic DNA from the same three isolates. Relative percentages of the RF copy number in each fraction were determined by dividing individual RF peak heights by the sum of the peak heights. Table S6 in the supplemental material shows a sample calculation from one of the fractions in the ^{15}N gradient demonstrating how the qPCR values shown in Fig. 2A were distributed among the various populations (Fig. 2B to F). RF quantities for each fraction were determined by multiplying the relative numbers by the total number of bacterial 16S rRNA genes. If a species had multiple peaks, the peaks were summed. Figure 2

shows the abundance of 16S rRNA amplicons as a function of BD: total 16S rRNA genes (Fig. 2A), RFs for *E. coli* 16S rRNA genes (Fig. 2B), RFs for *Rhodococcus rhodochrous* 11Y 16S rRNA genes (Fig. 2C), RFs for *Microbacterium* sp. MA1 16S rRNA genes (Fig. 2D), and two RFs from the soil selected for their apparent variations in G+C content (Fig. 2E and F).

Figure 2B to D show clear shifts in the RF peaks of the added ^{15}N -DNA (gray lines) relative to the RF profiles of the unlabeled DNA (black lines). In contrast, the two RF profiles of indigenous bacteria in the unlabeled soil DNA (Fig. 2E and F) were not shifted in the gradient with ^{15}N -labeled DNA from the isolates. The shifts of the diagnostic 16S rRNA gene RFs presented in Fig. 2B to F were quantified by calculating differences in buoyant density values between gradients at the RF profile maximums. The calculated buoyant density increases for the RFs in Fig. 2B to F are presented in Table 3. The efficiency of DNA recovery from the fractions was not factored into the calculations. Examination of the purification method used indicated that DNA recovery efficiency decreased as DNA concentrations fell below ca. $200 \mu\text{g} \mu\text{l}^{-1}$ (data not shown). However, this decreased efficiency would not be expected to alter the RF BD calculations presented in Table 3. The shifts observed in the three genomic DNA samples are similar to the predicted shift of 0.016 g ml^{-1} (6).

A direct comparison of the qPCR-TRFLP method to commonly used methods for comparing RF distributions demonstrated its improvement over the conventional approaches (Fig. 3). Although the position of some of the RF peaks could be deciphered from direct TRFLP analysis (e.g., the *E. coli* position) (data not shown), others could not. Figure 3A through C compare alternative methods to determine the position of RF 144. Figure 3A presents RF 144 relative peak height values normalized by maximum height, as commonly used in published ^{15}N SIP analyses (7). Figure 3B displays the relative peak heights normalized using the sum of all peak values from each chromatogram. Figure 3C is an analysis of peak position using the qPCR-TRFLP protocol. The same comparison of analysis methods was made for the RFs specific for *Microbacterium* sp. MA1 (Fig. 3D to F). Using the RF abundance (Fig. 3C and F), the distributions of these two populations along the gradients were clearly resolved, and the buoyant density shift of MA1 indicative of ^{15}N assimilation was observed.

DISCUSSION

The main objective of this study was to advance SIP analysis by developing a sensitive and robust method for measuring copy number of specific OTUs at different buoyant densities, a modification essential for assessing minor changes due to partial ^{13}C

TABLE 3 Calculated buoyant density shifts of peaks between the unlabeled and ^{15}N profiles^a

Source	Maximum BD (g ml^{-1})		BD shift (g ml^{-1})
	^{14}N gradient	^{15}N gradient	
<i>E. coli</i> K-12 MG1655	1.713	1.730	0.017
<i>R. rhodochrous</i> 11Y	1.728	1.745	0.017
<i>Microbacterium</i> sp. MA1	1.724-1.728	1.741	0.013-0.017
Soil RF 40	1.704-1.707	1.705-1.709	0.001-0.005
Soil RF 144	1.724	1.726-1.730	0.002-0.006

^a Peaks correspond to those presented in Fig. 2A to F. Maximum BD values were derived from the fractions with the maximum RF copy numbers. A range is provided where a clear maximum was not observed.

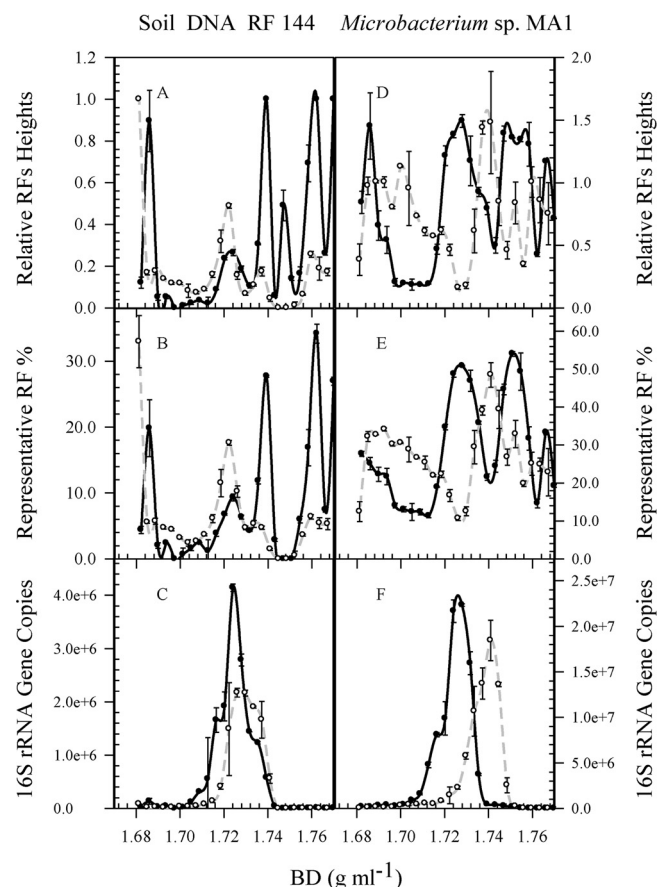


FIG 3 Stable isotope probing (SIP) profiles of soil DNA peak 144 and RFs of *Microbacterium* sp. MA1 in the buoyant density gradients determined by three methods. (A and D) SIP profiles of relative RF values (RF peak heights divided by the largest RF of each chromatogram; values in panel D rise above 1 due to multiple RF peaks of MA1 summed). (B and E) SIP profiles of relative peak heights (RFs % of total peak heights). (C and F) SIP profiles of RF copy numbers (values in panels B and E multiplied by respective qPCR values from each reaction).

incorporation or any degree of ^{15}N labeling of DNA. In brief, the fluorescence intensity of EvaGreen provided for highly sensitive quantification not compromised by inclusion of a fluorescein-labeled primer ([6'-FAM]-27F) in the reaction mix. Although higher threshold values were needed to calculate C_T values with the inclusion of the labeled primer, the calculations derived at the respective threshold levels were comparable (Table 1). Subsequent testing with GM3 (25) or a 5-carboxy-2',4,4',5',7,7'-hexachlorofluorescein-modified version, 5-HEX-GM3 paired with 338R, displayed comparable baseline levels and no change in threshold was required for C_T calculation (data not shown). However, FAM is one of the most commonly used labels for TRFLP analysis, and recent tests comparing primers labeled with either FAM or HEX found that more OTUs could be identified using FAM (29). Additionally, many qPCR quantification software packages contain methods, such as the second derivative method (34), which calculate a crossing-point value independent of the baseline. Despite the difference in G+C content of *E. coli* (50%) and *R. rhodochrous* (ca. 66%) in the genomic DNA mixes, TRFLP profiles were predictive of DNA mixture content (slopes within 0.1 of 1 and R^2 values > 0.98) (Table 3) when amplification was

held below 20 cycles. Slightly better results were achieved when the reaction was stopped closer to the C_T values (14, 30, 39). Abundance calculations based on relative peak height or relative peak area were comparable and would generally provide a useful cross-check in general sample analysis. Although greater deviation was observed between the amount of reference DNA added and the amount predicted from gradient profiles when it was mixed with soil DNA, the R^2 values remained consistently high. This observed difference would have little influence on the detection of minor shifts in density (Fig. 2).

The qPCR-TRFLP analysis applied to gradients with bisbenzamide, which increases the separation of DNA based on G+C content (6, 19), may possibly obviate the requirement for a second centrifugation step to identify minor populations in ^{15}N SIP (19). Unlike previous reports linking TRFLP analysis with real-time PCR (43), quantification using EvaGreen allows a wider range of applications, such as targeting multiple regions of the 16S rRNA gene and potentially quantifying changes within a community's functional gene diversity (4, 16). Similarly, quantification of amplicons using EvaGreen may make other fingerprinting analyses of density gradients more robust. For example, quantification should be possible prior to DGGE analyses of density gradients because the amplicons are often less than 400 bp (15, 20, 23, 33). EvaGreen is also suitable for high-resolution melting-curve analysis which can be used to verify amplification products or to expand community and gene diversity analyses (9, 24, 42). Finally, when used in conjunction with an unlabeled control gradient, the method can identify populations within a community having very small increases in buoyant density, as is associated with ^{15}N assimilation. Therefore, the method may have broad application to SIP analyses, allowing the identification of populations assimilating smaller amounts of ^{13}C isotopes than in previously reported SIP experiments.

ACKNOWLEDGMENTS

This research was funded by the Department of Defense Strategic Environmental Research and Development Program (SERDP; ER 1504).

We thank Chandhi Sun and the Stahl lab members for advice and assistance and Marina Kalyuzhnaya and the Lidstrom lab for use of equipment and support.

REFERENCES

- Addison SL, McDonald IR, Lloyd-Jones G. 2010. Stable isotope probing: technical considerations when resolving N-15-labeled RNA in gradients. *J. Microbiol. Methods* 80:70–75.
- Amann RI, et al. 1990. Combination of 16S ribosomal-RNA-targeted oligonucleotide probes with flow cytometry for analyzing mixed microbial-populations. *Appl. Environ. Microbiol.* 56:1919–1925.
- Andeer PF, Stahl DA, Bruce NC, Strand SE. 2009. Lateral transfer of genes for hexahydro-1,3,5-trinitro-1,3,5-triazine (RDX) degradation. *Appl. Environ. Microbiol.* 75:3258–3262.
- Bernhard AE, Donn T, Giblin AE, Stahl DA. 2005. Loss of diversity of ammonia-oxidizing bacteria correlates with increasing salinity in an estuary system. *Environ. Microbiol.* 7:1289–1297.
- Blattner FR, et al. 1997. The complete genome sequence of *Escherichia coli* K-12. *Science* 277:1453–1462.
- Buckley DH, Huangyutitham V, Hsu S-F, Nelson TA. 2007. Stable isotope probing with ^{15}N achieved by disentangling the effects of genome G+C content and isotope enrichment on DNA density. *Appl. Environ. Microbiol.* 73:3189–3195.
- Buckley DH, Huangyutitham V, Hsu SF, Nelson TA. 2007. Stable isotope probing with $^{15}\text{N}_2$ reveals novel noncultivated diazotrophs in soil. *Appl. Environ. Microbiol.* 73:3196–3204.
- Cadisich G, et al. 2005. Technical considerations for the use of N-15-DNA

- stable-isotope probing for functional microbial activity in soils. *Rapid Commun. Mass Spectrom.* 19:1424–1428.
9. Cheng J-C, et al. 2006. Rapid detection and identification of clinically important bacteria by high-resolution melting analysis after broad-range ribosomal RNA real-time PCR. *Clin. Chem.* 52:1997–2004.
 10. Culman SW, Gauch HG, Blackwood CB, Thies JE. 2008. Analysis of T-RFLP data using analysis of variance and ordination methods: a comparative study. *J. Microbiol. Methods* 75:55–63.
 11. Cupples AM, Shaffer EA, Chee-Sanford JC, Sims GK. 2007. DNA buoyant density shifts during N-15-DNA stable isotope probing. *Microbiol. Res.* 162:328–334.
 12. Dehal PS, et al. 2010. MicrobesOnline: an integrated portal for comparative and functional genomics. *Nucleic Acids Res.* 38:D396–D400.
 13. Dong D, Yan A, Liu H, Zhang X, Xu Y. 2006. Removal of humic substances from soil DNA using aluminum sulfate. *J. Microbiol. Methods* 66:217–222.
 14. Egert M, Friedrich MW. 2003. Formation of pseudo-terminal restriction fragments, a PCR-related bias affecting terminal restriction fragment length polymorphism analysis of microbial community structure. *Appl. Environ. Microbiol.* 69:2555–2562.
 15. Griffiths RI, Whiteley AS, O'Donnell AG, Bailey MJ. 2003. Influence of depth and sampling time on bacterial community structure in an upland grassland soil. *FEMS Microbiol. Ecol.* 43:35–43.
 16. Horz HP, Yimga MT, Liesack W. 2001. Detection of methanotroph diversity on roots of submerged rice plants by molecular retrieval of *pmoA*, *mmoX*, *mxoF*, and 16S rRNA and ribosomal DNA, including *pmoA*-based terminal restriction fragment length polymorphism profiling. *Appl. Environ. Microbiol.* 67:4177–4185.
 17. Hou Y, Zhang H, Miranda L, Lin S. 2010. Serious overestimation in quantitative PCR by circular (supercoiled) plasmid standard: microalgal *pcna* as the model gene. *PLoS One* 5:e9545.
 18. Kalyuzhnaya MG, et al. 2008. High-resolution metagenomics targets specific functional types in complex microbial communities. *Nat. Biotechnol.* 26:1029–1034.
 19. Karlovsky P, Decock A. 1991. Buoyant density of DNA Hoechst-33258 (bisbenzimidazole) complexes in CsCl gradients—Hoechst-33258 binds to single AT base-pairs. *Anal. Biochem.* 194:192–197.
 20. Kasai Y, Takahata Y, Manefield M, Watanabe K. 2006. RNA-based stable isotope probing and isolation of anaerobic benzene-degrading bacteria from gasoline-contaminated groundwater. *Appl. Environ. Microbiol.* 72:3586–3592.
 21. Lane DJ. 1991. 16S/23S rRNA sequencing, p. 115–175. In Stackebrandt E and Goodfellow M (ed), *Nucleic acid techniques in bacterial systematics*. John Wiley and Sons, New York, NY.
 22. Lueders T, Pommerenke B, Friedrich MW. 2004. Stable-isotope probing of microorganisms thriving at thermodynamic limits: syntrophic propionate oxidation in flooded soil. *Appl. Environ. Microbiol.* 70:5778–5786.
 23. Manefield M, Whiteley AS, Griffiths RI, Bailey MJ. 2002. RNA stable isotope probing, a novel means of linking microbial community function to phylogeny. *Appl. Environ. Microbiol.* 68:5367–5373.
 24. Mao F, Leung WY, Xin X. 2007. Characterization of EvaGreen and the implication of its physicochemical properties for qPCR applications. *BMC Biotechnol.* 7:76.
 25. Muyzer G, Teske A, Wirsén CO, Jannasch HW. 1995. Phylogenetic relationships of *Thiomicrospira* species and their identification in deep-sea hydrothermal vent samples by denaturing gradient gel-electrophoresis of 16S rDNA fragments. *Arch. Microbiol.* 164:165–172.
 26. Neufeld JD, Chen Y, Dumont MG, Murrell JC. 2008. Marine methylotrophs revealed by stable-isotope probing, multiple displacement amplification and metagenomics. *Environ. Microbiol.* 10:1526–1535.
 27. Neufeld JD, et al. 2007. DNA stable-isotope probing. *Nat. Protoc.* 2:860–866.
 28. Osterman LA. 1984. *Methods of protein and nucleic acid research*. Springer-Verlag, Berlin, Germany.
 29. Pandey J, Ganesan K, Jain RK. 2007. Variations in T-RFLP profiles with differing chemistries of fluorescent dyes used for labeling the PCR primers. *J. Microbiol. Methods* 68:633–638.
 30. Polz MF, Cavanaugh CM. 1998. Bias in template-to-product ratios in multitemplate PCR. *Appl. Environ. Microbiol.* 64:3724–3730.
 31. Radajewski S, Ineson P, Parekh NR, Murrell JC. 2000. Stable-isotope probing as a tool in microbial ecology. *Nature* 403:646–649.
 32. Radajewski S, et al. 2002. Identification of active methylotroph populations in an acidic forest soil by stable isotope probing. *Microbiology (UK)* 148:2331–2342.
 33. Rangel-Castro JI, et al. 2005. Stable isotope probing analysis of the influence of liming on root exudate utilization by soil microorganisms. *Environ. Microbiol.* 7:828–838.
 34. Rasmussen R. 2001. Quantification on the Lightcycler, p 21–34. In Meurer S, Wittwer C, and Nakagawara K (ed), *Rapid cycle real-time PCR, methods and applications*. Springer Press, Heidelberg, Germany.
 35. Sambrook J, Russell DW. 2001. *Molecular cloning: a laboratory manual*, 3rd ed. Cold Spring Harbor Laboratory Press, Cold Spring Harbor, NY.
 36. Schwartz E. 2007. Characterization of growing microorganisms in soil by stable isotope probing with H₂¹⁸O. *Appl. Environ. Microbiol.* 73:2541–2546.
 37. Schwarz S, Waschowitz T, Daniel R. 2006. Enhancement of gene detection frequencies by combining DNA-based stable-isotope probing with the construction of metagenomic DNA libraries. *World J. Microbiol. Biotechnol.* 22:363–367.
 38. Seth-Smith HMB, et al. 2002. Cloning, sequencing, and characterization of the hexahydro-1,3,5-trinitro-1,3,5-triazine degradation gene cluster from *Rhodococcus rhodochromus*. *Appl. Environ. Microbiol.* 68:4764–4771.
 39. Suzuki MT, Giovannoni SJ. 1996. Bias caused by template annealing in the amplification of mixtures of 16S rRNA genes by PCR. *Appl. Environ. Microbiol.* 62:625–630.
 40. von Wintzingerode F, Gobel UB, Stackebrandt E. 1997. Determination of microbial diversity in environmental samples: pitfalls of PCR-based rRNA analysis. *FEMS Microbiol. Rev.* 21:213–229.
 41. Wawrik B, Callaghan AV, Bronk DA. 2009. Use of inorganic and organic nitrogen by *Synechococcus* spp. and diatoms on the West Florida Shelf as measured using stable isotope probing. *Appl. Environ. Microbiol.* 75:6662–6670.
 42. White HE, Hall VJ, Cross NCP. 2007. Methylation-sensitive high-resolution melting-curve analysis of the SNRPN gene as a diagnostic screen for Prader-Willi and Angelman syndromes. *Clin. Chem.* 53:1960–1962.
 43. Yu CP, Ahuja R, Saylor G, Chu KH. 2005. Quantitative molecular assay for fingerprinting microbial communities of wastewater and estrogen-degrading consortia. *Appl. Environ. Microbiol.* 71:1433–1444.